Pure appl. geophys. 163 (2006) 2389–2406
0033–4553/06/122389–18
DOI 10.1007/s00024-006-0129-8

Pure and Applied Geophysics

Acoustic Emission Experiments of Rock Failure Under Load Simulating the Hypocenter Condition

Hui-hui Zhang,[1,6] Xiang-chu Yin,[1,2,3] Nai-gang Liang,[1] Huai-zhong Yu,[1] Shi-yu Li,[3] Y.C. Wang,[4] C. Yin,[4] Victor Kukshenko,[5] Nikita Tomiline,[5] and Surguei Elizarov[6]

Abstract—A series of acoustic emission (AE) experiments of rock failure have been conducted under cyclic load in tri-axial stress tests. To simulate the hypocenter condition the specimens are loaded by the combined action of a constant stress, intended to simulate the tectonic loading, and a small sinusoidal disturbance stress, analogous to the Earth tide induced by the Sun and the Moon. Each acoustic emission signal can indicate the occurrence time, location and relative magnitude of the damage (micro-crack) in the specimen. The experimental results verified some precursors such as LURR (Load/Unload Response Ratio) and AER (Accelerating Energy Release) before macro-fracture of the samples. A new parameter, the correlation between the AE and the load, has been proposed to describe the loading history. On the eve of some strong earthquakes the correlation between the Benioff strain and the Coulomb failure stress (CFS) decreases, similar to the variation of LURR prior to strong earthquakes.

Key words: Acoustic emission (AE), cyclic load, load/unload response ratio (LURR), critical point hypothesis (CPH), accelerating energy release (AER), correlation (Corr).

Introduction

In recent years many investigators have attempted to use the methods of statistical physics to understand regional seismicity (Rundle, 1988a,b; 1989a,b). One approach has been put forward to model the earthquake process as a critical phenomenon (Sornette and Sornette, 1990; Sornette and Sammis, 1995; Bowman *et al.*, 1998; Rundle *et al.*, 1999; Huang, 1998; Ito, 1990). According to

[1] LNM (State Key Laboratory of Nonlinear Mechanics), Institute of Mechanics, CAS (Chinese Academy of Sciences), Beijing, 100080. E-mail: zhanghh@lnm.imech.ac.cn
[2] Institute of Earthquake Prediction, China Seismological Bureau, Beijing 100036. E-mail: xcyin@public.bta.net.cn
[3] Institute of Geophysics, China Seismological Bureau, Beijing, 100081, China.
[4] QUAKES, Department of Earth Sciences, The University of Queensland, Brisbane, 4072, Australia. E-mail: wangyc@esscc.uq.edu.au
[5] Ioffe Physical Technique Institute, Russian Academy of Sciences, Russia. E-mail: Victor.Kuksenko@pop.ioffe.ssi.ru
[6] School of Civil Engineering and Mechanics, Yanshan University, China, 066004.

the Critical Point Hypothesis (CPH), the earth's crust does not remain perpetually in or near a critical state, but repeatedly approaches and retreats from a critical state. The critical point hypothesis for large earthquakes predicts two different precursory phenomena in space and time, an accelerating moment release and the growth of the spatial correlation length between its different parts. XIA *et al.* (2002) presented critical sensitivity and trans-scale fluctuations associated with catastrophic rupture in a system. Critical sensitivity means that the system becomes significantly sensitive near the catastrophe transition. This could lead to triggering of earthquakes by tidal stress (GRASSO and SORNETTE, 1998) and consequently anomalously high values of LURR (YIN and YIN, 1991; YIN, 1993; Yin *et al.*, 1994–2000, 2002) are observed prior to strong earthquakes. The establishment of long-range correlations in the regional stress field (SAMMIS and SMITH, 1999; MORA and PLACE, 2000, 2002; WEATHERLEY, 2002) and accelerating seismic activity of moderate-sized earthquakes (ELLSWORTH *et al.*, 1981; KEILIS-BOROK, 1990; SORNETTE and SAMMIS, 1995; KNOPOFF *et al.*, 1996 and BOWMAN *et al.*, 1998) and equivalently, the accelerating seismic release prior to large earthquakes follows a power-law time-to-failure formula. LURR and AER reflect the changing critical sensitivity and growing correlation length before large earthquakes, respectively.

It is recognized by many scientists that, from the viewpoint of physics, earthquake is the failure or instability of the focal media accompanied by a rapid release of energy. Similarly, the acoustic emissions in rock experiment are elastic waves generated in conjunction with energy release during crack onset and propagation and internal deformations in the rock body. Laboratory experiments of rock deformation are considered as a tool for understanding the occurrence of natural earthquakes. By recording AE during a laboratory test of rock samples, significant additional information of the failure process can be obtained. Information about the onset and propagation of micro-cracking and fracture in rock samples, subjected to different stress regimes can be determined by recording the time and location of AE during the test. Using AE to map out fault nucleation and propagation may also be useful in understanding earthquake mechanisms and may contribute to solving the problem of earthquake prediction (LOCKNER *et al.*, 1991).

The main motivation of our work is to investigate the fracture precursors of heterogeneous brittle material. We are going to monitor the acoustic emission (AE) from micro-fractures that occur before the final fracture, and test LURR and AER using acoustic emission data recorded during rock fracture experiments.

Experimental Setup and Procedures

The experiment designed for this research program utilizes large rectangular prisms, rock samples. The samples include sandstone from Chengdu City, Sichuan Province, and gneiss from Jinzhou City, Liaoning Province. The dimensions

of Chengdu sandstone and Jinzhou gneiss are $300 \times 360 \times 20\,\mathrm{mm}^3$ and $300 \times 360 \times 25\,\mathrm{mm}^3$, respectively. The other parameters for Jinzhou gneiss are: Young's modulus $E = 27$ Gpa, Possion ratio $v = 0.26$, density $\rho = 2.6 \times 10^3\,\mathrm{kg/m}^3$, and longitudinal sound velocity $v = 2900\,\mathrm{m/s}$; and for Chengdu sandstone: Young's modulus of $E = 19$ GPa, Possion ratio $v = 0.26$, density $\rho = 2.5 \times 10^3\,\mathrm{kg/m}^3$ and longitudinal sound velocity $v = 1500\,\mathrm{m/s}$.

The experiments are conducted using MTS-100 servo-control experimental equipment in Institute of Geophysics, China Seismological Bureau. The maximum load for this facility is 100 ton in axial direction and 30 ton in lateral direction. Boundary-displacement control is used to load the system until final failure. Samples are subjected to both axial stress σ_1 and lateral load σ_2 simultaneously and another principle stress σ_3 is zero. The greatest, intermediate and least principle stress are $\sigma_1, \sigma_2, \sigma_3$. So that:

$$\sigma_1 \neq \sigma_2 \neq \sigma_3.$$

Therefore, the stress state is a tri-axial stress state (Fig. 1). Under such a stress state all of the specimens undergo shear failure at the last stage.

In our experiments the lateral stress σ_2 is symmetrically applied to samples with steel plates on the two smaller sides of the specimens and it keeps constant until the samples fracture. Then the axial stress σ_1 is applied.

σ_1 consists of two parts: The constant loading rate of tectonic stress build-up and a sinusoidal stress perturbation which simulates the periodic loading and unloading

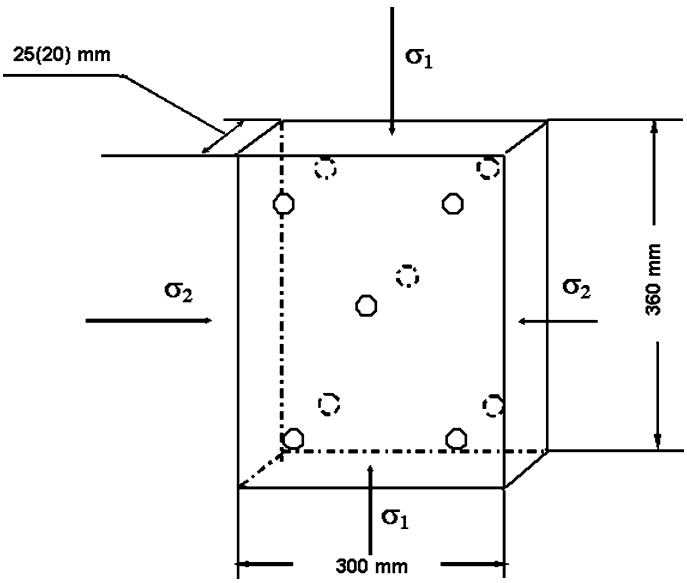

Figure 1
The Geometry of the specimens, the loading conditions, and the arrangement of AE sensors (circles).

Figure 2 ▶

The loading history and the corresponding experimental results for gneiss specimen G2. The average loading velocity is 0.4 μm/s. (a) The loading history in the experiment for gneiss specimen G2. P1 is the axial load. The amplitude and the periodicity of the cyclic period loading cycles is 200 kg and 50 s, respectively. P2 is the lateral load and it keeps 10 tons during the entire course. (b) The AE event rate versus time for gneiss specimen G2. (c) The AE energy rate versus time for gneiss specimen G2.

cycles induced by tidal forces. During the early stage of seismogenic process, which is a prolonged period before the occurrence of a large earthquake and maybe several or dozens of years, the tectonic stress level is low. Subsequently, tectonic loading drives the crust towards the critical state. During the establishment of criticality, the crust in this region is damaged severely after which the crust will be sensitive to any tiny external disturbance, such as tidal stress whose minimum period is only a dozen hours. Thus the tidal stress period is only a very small fraction of the entire reoccurrence time between two strong earthquakes. On the other hand, it is well known that the resultant stress σ_{ij} in the crust consists of tectonic stress σ_{ij}^T and the tide induced stress σ_{ij}^t. Although the level of σ_{ij}^T in the crust (in the order of 10^6–10^8 Pa) is considerably higher than the level of σ_{ij}^t (10^3–10^4 Pa), the change rate of tidal-induced stress is considerably larger than the change rate of the tectonic stress (VIDALI *et al.*, 1998). Since the tidal stress period is small compared to the whole reoccurrence time between two strong earthquakes.

The loading history of gneiss sample G2 is shown in Figure 2(a). P_2 is the lateral load which keeps constant (10 ton) during the loading until the samples fracture. The axial load, P_1, increases to a certain value (33 ton) and then cyclic loading is added until the final fracture. The amplitude (200 kg) and the periodicity (50 sec) of the cyclic loading cycles are enlarged in the circle for more details. Figure 3(a) is the loading history of sandstone sample S1.

The acoustic emission equipment (12 digits, 32 channels) of Ioffe Physical Technique Institute, Russian Academy of Science is used to keep a continuous log (recording) of the time, location and intensity of micro-cracks within rock samples. Each channel consists of an AE sensor, a preamplifier and an AECB (Acoustic Emission Channel Board). The AE sensors pick up the sound waves from the specimens and convert them into an electrical signal that is then amplified by a preamplifier and converted into a digital data stream in an AECB. AE features such as arrival times, rise-times, duration, peak amplitude, energy and counts are extracted by a FPGA (Field Programmable Gate Array). Since an AE event is generally corresponding to a micro-cracking, AE hypocenter distribution reflects directly the distribution of micro-cracking. The rapid AE monitoring system can record AE waveforms without major loss of events, even for AE event rate on the order of several thousand events per second. Ten piezoelectric transducers (resonance from 50 to 250 kHz) are attached directly to the rock sample surface ('o' represents the location of transducers in Fig. 1), five on each side. They are used to monitor the high-frequency acoustic emissions generated in the sample as it is stressed. The

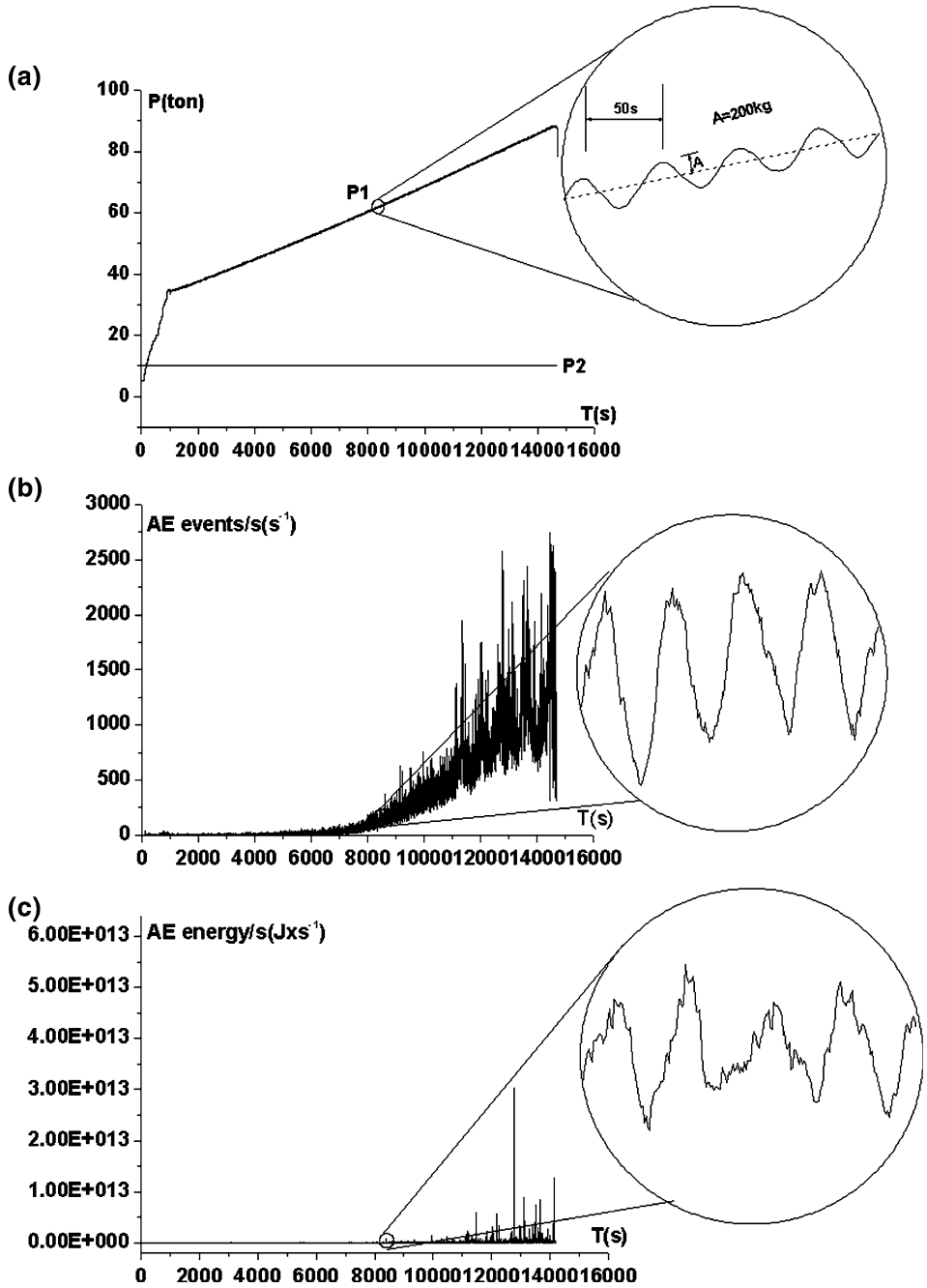
(a)
P(ton)
100
80
60
40
20
0
P1
P2
T(s)
0 2000 4000 6000 8000 10000 12000 14000 16000
50s
A=200kg
TA
(b)
AE events/s(s-1)
3000
2500
2000
1500
1000
500
0
T(s)
0 2000 4000 6000 8000 10000 12000 14000 16000
(c)
AE energy/s(Jxs-1)
6.00E+013
5.00E+013
4.00E+013
3.00E+013
2.00E+013
1.00E+013
0.00E+000
T(s)
0 2000 4000 6000 8000 10000 12000 14000 16000

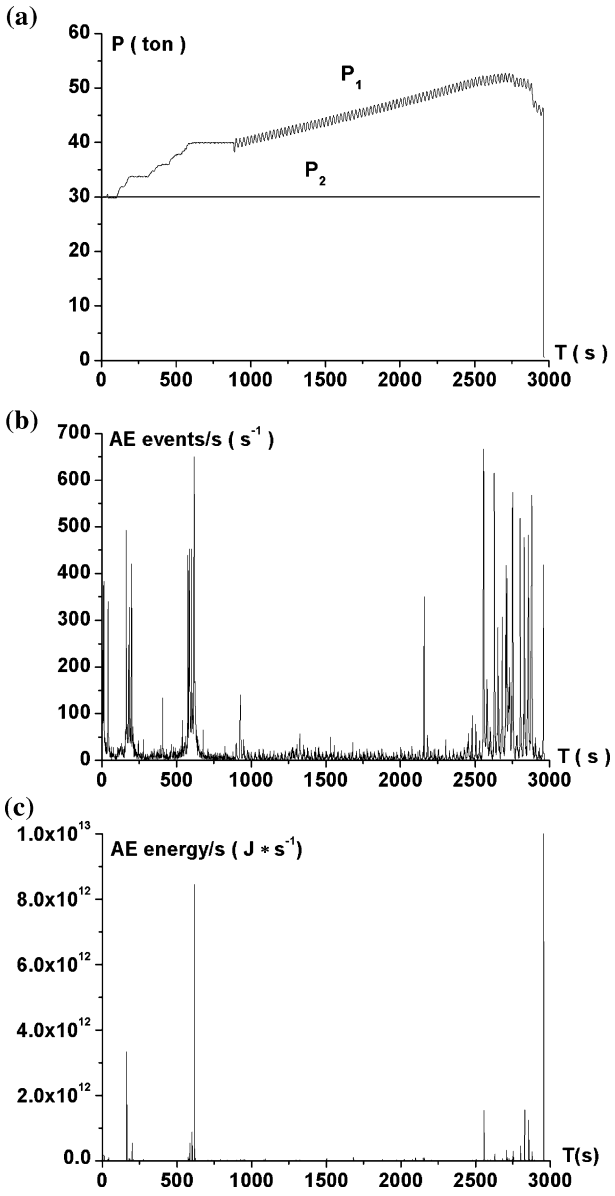

Figure 3

The loading history and the corresponding experimental results for sandstone specimen S1. The average loading velocity is 0.3 μm/s. (a) The loading history in the experiment for sandstone specimen S1. P1 is the axial load. The amplitude and the periodicity of the cyclic period loading cycles is 300 kg and 25 s, respectively. P2 is the lateral load and it is 30 tons during the whole course. (b) The AE event rate versus time for sandstone specimen S1. (c) The AE energy rate versus time for sandstone specimen S1.

nucleation and growth of micro-cracks are represented by AE event. Thus we are able to investigate the nucleation and growth of fracture by acquiring and analyzing AE signals (LOCKNER *et al.*, 1991, 1993; TOMILIN *et al.*, 1994).

Experimental Results

The experiments have been conducted by 20 scientists from three countries (China, Russia and Australia) during 40 days. For each specimen millions of AE events have been recorded, among which thousands of events can be located. Figures 2 (b,c) and Figures 3 (b,c) are the AE records versus time for gneiss specimen G_2 and sandstone S_1, respectively. At the early stage of the loading there are few micro-fractures in the samples so the AE event rate and energy rate are relatively low. With increasing stress, more and larger micro-cracks appear and some micro-cracks coalesce into larger cracks which lead to increased AE event rate and energy rate. Thereafter additional and larger AE events concentrate before the macro-fracture of the samples.

The acquired AE data allow us to examine the details concerning the appearance and localization of micro-cracks. Figure 4 shows the plots of the spatial distribution of AE hypocenters during different stages. In the beginning micro-fractures are roughly uniformly distributed. Afterwards they begin to concentrate and to nucleate, eventually producing a major fault with the increasing pressure, followed by the final catastrophic failure. This phenomenon has also been observed experimentally by many people such as Lockner *et al.* in granite samples undergoing monotonic loading (LOCKNER *et al.*, 1991; LOCKNER 1993). They distinguish three stages in the process: randomly distributed micro-fractures, nucleation and growth of the nucleation sites. Our experiment supports this feature. Besides, other quantities such as LURR and AER have also been obtained.

YIN and YIN (1991), YIN (1993), YIN *et al.* (1994, 1995, 2000, 2002) proposed an approach called the Load-Unload Response Ratio (LURR) to test for the crustal criticality. It is defined as

$$Y = \frac{X_+}{X_-}, \tag{1}$$

where X_+ and X_- are the response rates during loading and unloading according to some measure.

The idea that motivated the LURR earthquake prediction approach is that when a system is in elastic regime, its response to loading is nearly the same as its response to unloading, whereas the response to loading and unloading becomes quite different when the system is in the damage regime. The ratio of the response to loading and unloading can measure quantitatively the damage extent.

It is clear that $Y = 1$ for the elastic regime since $X_+ = X_-$ and $Y > 1$ for the damage regime due to $X_+ > X_-$. The more severely damaged the material, the larger

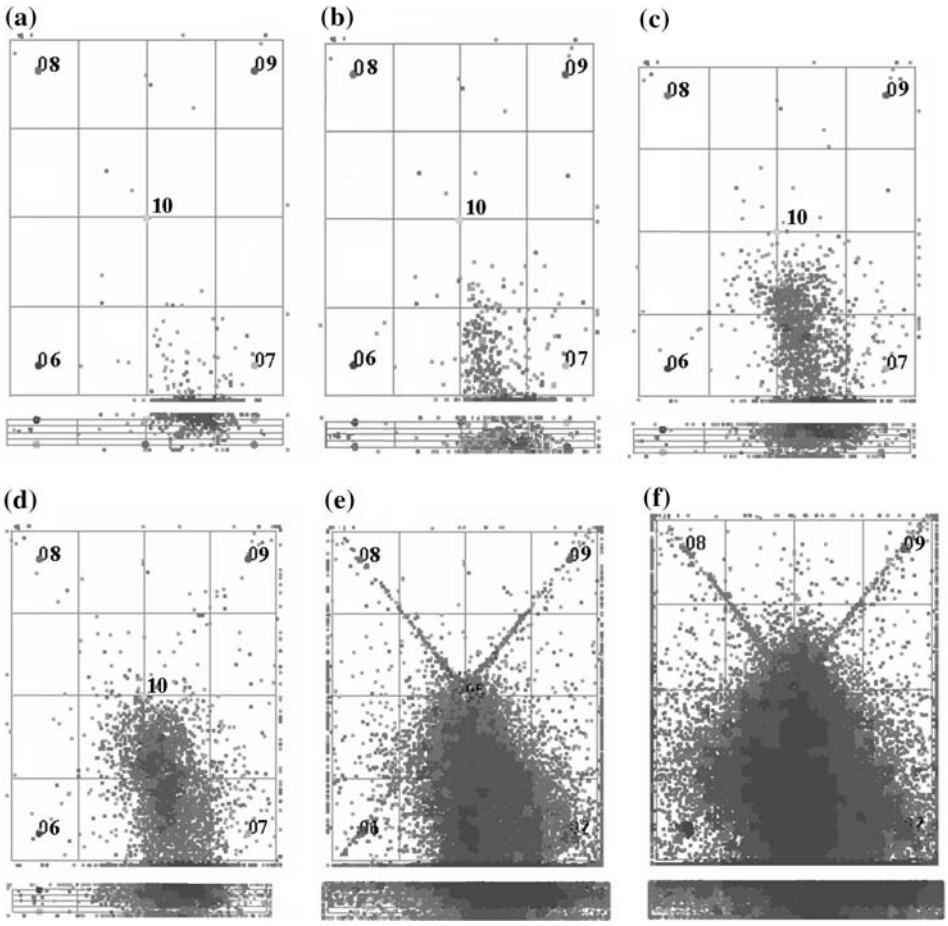

Figure 4
Evolution of damage in terms of the AE hypocenters location with the increasing load. Micro-fractures detected in each interval are represented in plots (a)–(e) (increasing stress). In (f) all the micro-fractures are plotted. The upper picture is seen from the front side and the lower one is seen from the top.

the Y value will become. As the media approach failure the Y value becomes increasingly larger so that the Y value could measure the proximity to failure and also acts as a precursor for earthquake prediction.

In order to predict earthquakes by means of the parameter LURR several main problems need to be solved. One is how to load and unload a block of crust and how to distinguish loading from unloading. The linear dimension of a seismogenic zone may reach hundreds even thousands of kilometers. One of the means to load and unload is by the earth's tide. Tidal force varies periodically, so the induced stresses in the crust continue to loading and unloading it periodically. To distinguish loading from unloading for rock materials in the three-dimensional stress state, we resort to

the Coulomb failure criterion (RESERNBERG and SIMPSON, 1992; HARRIS, 1998). It can be expressed as the following:

$$CFS = \tau_n + f\sigma_n, \tag{2}$$

where τ_n and σ_n are shear and normal stress resolved on the fracture plane. f is the coefficient of inner friction. n is the normal of the fault plane on which the CFS reaches its maximum. ΔCFS is the increment of CFS. If the increment of Coulomb failure stress $\Delta CFS > 0$, it is referred to as loading; otherwise $\Delta CFS < 0$ is referred to as unloading.

When calculating CFS the total stress tensor at every point in the earth's crust, including tectonic stress σ_T and tidal stress σ_t, is used. As to the tectonic stress field, we mainly use the results of ZHONGHUAI XU *et al.* for Chinese Mainland (ZHONGHUAI XU *et al.,* 1995), and Mary Lou Zoback's results for other regions (http://www.world-stress-map.org/). On the basis of Molodensksy-Takeuchi's work, we independently wrote the code of calculating stress tensor at any point in the earth's crust. The shear and normal stresses on the fault plane with normal n can be obtained by stress tensor transform and subsequently the CFS can be calculated easily according to (2).

High LURR values indicate that a region is prepared for a strong earthquake. In previous years, a series of successful intermediate-term predictions have been made for strong earthquakes in China and other countries. In LURR theory, Y is defined directly by the released seismic energy as follows:

$$Y_m = \frac{\left(\sum_{i=1}^{N^+} E_i^m\right)_+}{\left(\sum_{i=1}^{N^-} E_i^m\right)_-}, \tag{3}$$

where E denotes released seismic energy, the sign "+" means loading and "–" means unloading, $m = 0$ or $1/3$ or $1/2$ or $2/3$ or 1. For $m = 1$, E^m is exactly the energy itself; for $m = 1/2$, E^m denotes the Benioff strain; for $m = 1/3, 2/3$, E^m represents the linear scale and area scale of the focal zone, respectively; for $m = 0$, Y is equal to N^+/N^-, where N^+ and N^- denote the number of earthquakes occurring during the loading and unloading periods, respectively. In general m is chosen as $1/2$, which means that Y is determined by Benioff strain during the loading and unloading period. While the LURR reaches a high value several months or years prior to the occurrence of strong earthquakes, on the eve of strong earthquakes the LURR decreases to a low level and then the large event occurs.

According to our understanding, the peak-point of the LURR curve suggests the formation of macro-crack in loaded rock specimens (JAEGER, and COOK, 1979) or the beginning of nucleation of an earthquake. After that the system will evolve into the so called self-driving stage, which means that it will obey its own evolution law

(fracture dynamics) and the system is no longer sensitive to the external disturbance. Therefore the LURR decreases to a low level before the large event occurs. XIA *et al.,* (2002) presented critical sensitivity to describe the damage evolved in materials. The numerical simulation of the damage and fracture process for brittle inhomogeneous material also shows a peak of sensitivity prior to the catastrophic rupture which is similar to the variation of LURR (ZHANG *et al.,* 2004). According to Beeler and Lockner's result the minimum typical duration of earthquake nucleation on the San Andreas fault system is about 1 year (BEELER and LOCKNER, 2003) which is in a good agreement with our results.

In our experiment AE energy is used to calculate LURR. The true AE energy is directly related to the area under the acoustic emission waveform which in turn can be measured by digitizing and integrating the waveform signal. As a simplification, the AE event energy can be approximated as the square of the peak amplitude (LOCKNER *et al.*, 1991). The resulting values are actually more representative of the intensity of the event but are commonly referred to as energy calculations in the AE literature. This is due to their approximately linear relationship with energy (the units of this term are given in decibels or dB, which can be defined as 10 times the logarithm, to the base 10, of the ratio of two mean square values of voltage). The main reason to perform this type of "energy" analysis is to accentuate events with abnormally large amplitudes. This type of energy measurement is not an absolute energy, but a relative quantity proportional to the true energy.

The results of LURR in this experiment are shown in Figure 5. The arrows indicate the failure time of the specimens. From Figure 5 we can see that at the beginning of the experiment LURR is low and fluctuates around 1. But prior to the final failure of the specimens, the LURR reaches a high value, then the LURR decreases prior to the occurrence of macro-fracture. The experimental results very favorably coincide with the seismological observations (YIN *et al.* 1994, 1995, 2000, 2002, *2004*)?

AER (Accelerating Energy Release)

Observational studies indicate that large earthquakes are sometimes preceded by phases of accelerated seismic release characterized by cumulative Benioff strain following a power-law time-to-failure relation. BUFE and VARNES (1993) and BUFE *et al.* (1994) found that the clustering of intermediate events before a large shock produces a regional increase in cumulative Benioff strain, $\varepsilon(t)$, which can be fit by a power-law time-to-failure relation of the form

$$\varepsilon(t) = A + B(t_c - t)^z \tag{4}$$

where t_c is the time of the large event, the constant A and B are fit parameters. The exponent z is set to 0.3 according to numerous AER studies, e.g., BUFE and VARNES

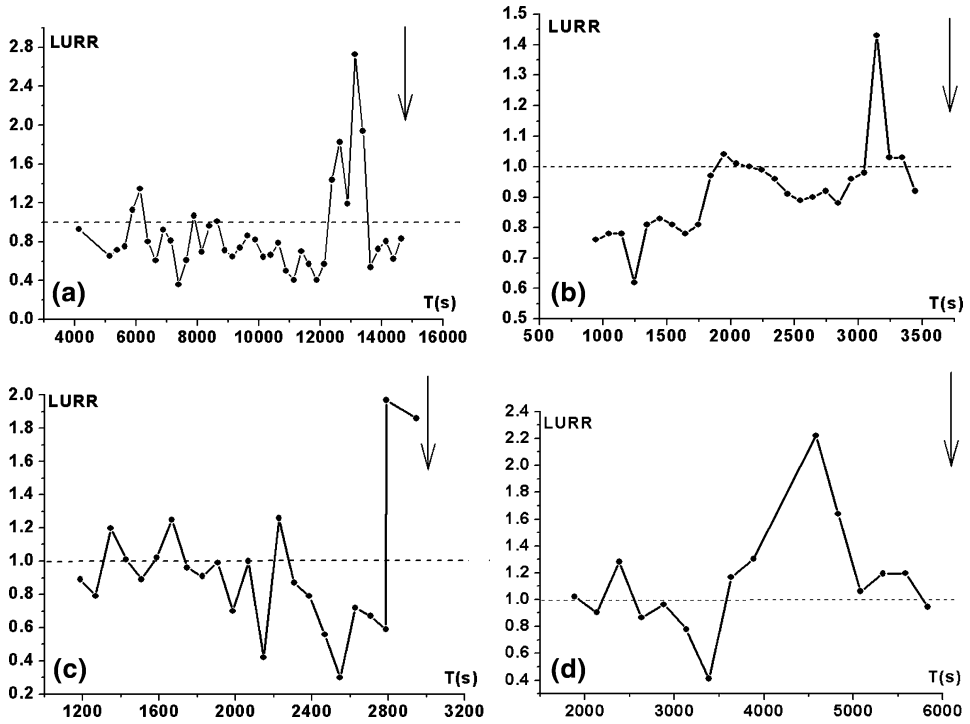

Figure 5
LURR anomaly during rock fracture experiments involving specimens: (a) gneiss G2, (b) gneiss G3, (c) sandstone S1, (d) sandstone S5.

(1993) and it is an exponent that defines the curvature of the power-law acceleration. A is the value of $\varepsilon(t)$ when $t = t_c$, i.e., the final Benioff strain up to and including the largest event. The cumulative Benioff strain at time t is defined as

$$\varepsilon(t) = \sum_{i=1}^{N(t)} E_i(t)^{1/2} \tag{5}$$

where E_i is the energy of the i-th event and $N(t)$ is the number of events at time t.

In order to quantify the degree of acceleration in the seismicity, a curvature parameter C is defined, where

$$C = \frac{\text{power-law fit root-mean-square error}}{\text{linear fit root-mean-square error}}. \tag{6}$$

Therefore when the data are best characterized by a power-law curve, the root-mean-square (RMS) error for the power-law fit will be small compared to the RMS error of the linear fit, C will be small. Conversely, if the seismicity linearly increases then the power-law fit will be statistically indistinguishable from a linear fit, the parameter C will be at or near unity.

The energy of AE event recorded in the experiment represented the elastic energy released by rock specimen. Thus we can investigate the evolution of elastic energy release of brittle materials by analyzing the energy of AE event. Figure 6 shows the experimental results for the specimens and the best fit to equation (4) for each specimen.

In this context the exponent z is in focus of the problem. SORNETTE (1992) found that the mean field value of the exponent z associated with a critical phase transition is $z = 1/2$. RUNDLE *et al.* (2000) used scaling arguments to show that power-law time-to-failure buildup of cumulative Benioff strain may represent the scaling regime of a spinodal phase transition, with an exponent $z = 1/4$. BEN-ZION and LYAKHOVSKY (2002) concluded that $z = 1/3$ for the damage rheology model of LYAKHOVSKY *et al.* (1997). TURCOTTE *et al.* (2002) used the discrete fiber-bundle model to investigate time-dependent failure of chipboard and fiberglass and obtained similar results. BEN-ZION and LYAKHOVSKY (2002) also listed the z value of seismological observations from various authors. The exponents fell in the range of 0.1 to 0.55 with the peak of the distribution at $z = 0.29$. In our experiment the measured z values

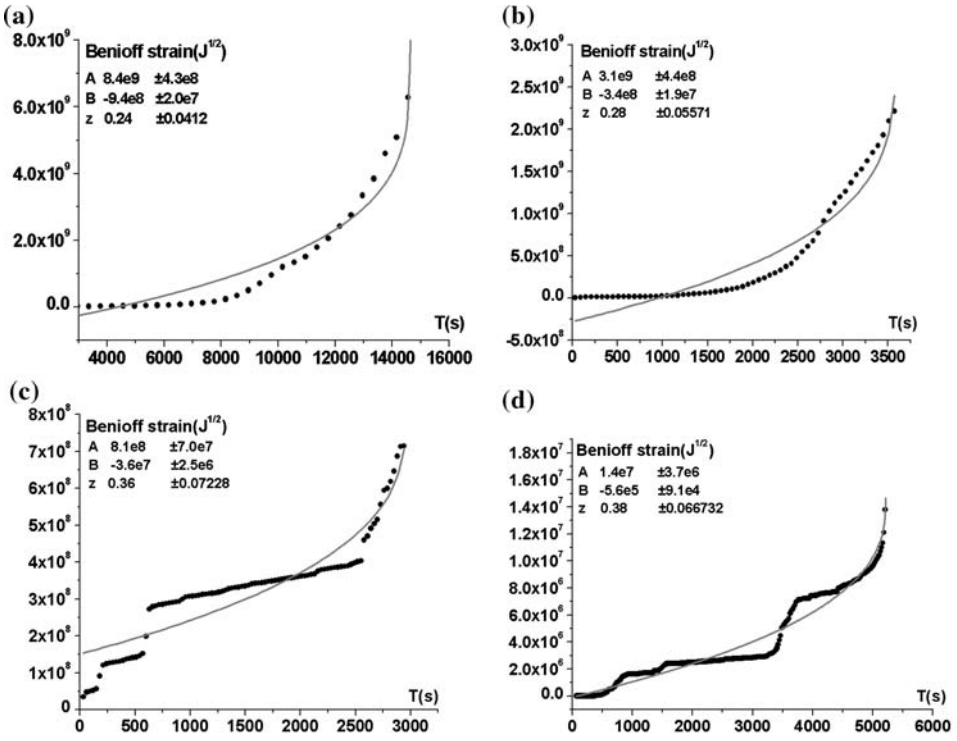

Figure 6
The AER curve prior to rock fracture for specimens: (a) gneiss G2, (b) gneiss G3, (c) sandstone S1, (d) sandstone S5.

are 0.24, 0.28, 0.36 and 0.38 for specimens gneiss G2, G3 and sandstone S1, S5, respectively, which is shown in Figure 6. These values fluctuate around 1/3. Our results are consistent with the results mentioned above.

On the other hand, the curvature parameter C is another focus of the problem. BOWMAN *et al.* (1998) tested the cumulative seismic strain release which increased as a power-law time to failure before large earthquakes in terms of the statistic physics of a critical phase transition. They found C fell in the range of 0.4 to 0.6 within the critical region. YUCANG WANG *et al.* (2003) analyzed the cumulative Benioff strain release preceding seven earthquakes with magnitudes above 5.0 in Australia since 1980. They found $0.45 \leq C \leq 0.65$ with z is about 0.3. In our experiment the curvature parameter C is 0.39, 0.53, 0.49 and 0.56 for specimens gneiss G2, G3 and sandstone S1, S5, respectively. Our results are consistent with the real earthquake results mentioned above.

The scatter in z and C values of our experiments is similar to that seen in observational earthquake data AER studies (BOWMAN *et al.*, 1998, YUCANG WANG *et al.*, 2003). The results confirm that energy release accelerates prior to macro-failure of the specimens and provide further support for the CPH. With the tidal stress the accelerating energy release is more significant than without that. Nonetheless until now no contrast tests have been conducted and further study is necessary to compare the difference of the behavior of the AER with and without tidal stress.

Correlation between the AE and Load

In our experiment the loading stress follows the formula below:

$$P = kt + A \sin \frac{2\pi}{T} t, \tag{7}$$

where k is rate of tectonic stress σ_{ij}^{T}, A and T are amplitude and period of the sinusoidal stress perturbation to simulating tidal stress.

During the experiment the obvious intense correlation between the AE and load is observed. At the beginning the AE event rate increases gradually with the increase of loading. At the intermediate and later loading stage the AE event rate in the specimen increases with the load increasing and decreases with the load decreasing. Many larger events appear and focus temporarily on the specimen. Figure 7 is the load and AE event rate versus time during the experiment. It is seen that the AE event rate increases when the load increases and decreases when the load decreases. A new parameter called the correlation between the AE and load has been put forward to describe the loading stage.

The correlation coefficient between the AE activity and load is

$$\mathrm{Corr} = \frac{\sum (P_i - \overline{P})(R_i - \overline{R})}{\sqrt{\sum (P_i - \overline{P})^2 \sum (R_i - \overline{R})^2}}, \tag{8}$$

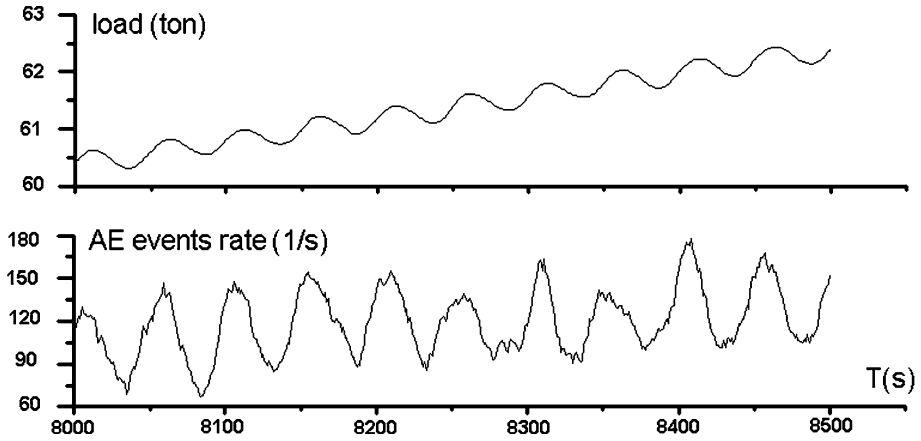

Figure 7
The load and AE events rate versus time during the loading of specimen gneiss G2.

where Corr is the correlation coefficient between P and R, P is the load and R is the AE event rate, $\overline{P}$, $\overline{R}$ is the average of P and R, respectively in the entire time window.

Using formula (8) we can get the correlation coefficient between the AE event rate and load of the specimens at different times. Figure 8 is the correlation between AE event rate and load versus time for specimen gneiss G2, G3 and sandstone S1, S5 respectively. At the outset of loading the Corr is very low. With the increase of the load the Corr also increases and reaches its peak value. However, before the fracture of the specimen the Corr decreases, which is similar to the variation of LURR with time.

Based on this phenomenon we have calculated the correlation between the Coulomb failure stress and the Benioff strain before two strong earthquakes; the results of which are show in Figure 9. The arrows denote the earthquake occurrence. Here the Coulomb failure stress is obtained as in LURR calculation. The results show that on the eve of the earthquakes the Corr falls down, exactly similar with LURR. This could be a new precursor of rock fracture and earthquake prediction.

Conclusions

In our experiment a series of rectangular prisms rock samples of sandstone and gneiss are stressed to failure under a cyclic load in tri-axial compression tests using acoustic emission (AE) monitoring. The experimental results show that high LURR (Load/Unload Response Ratio) and AER (Accelerating Energy Release) occur before the macro fracture of the specimens. These results are interpreted as evidence that brittle failure of heterogeneous media is a CP phenomenon. A new parameter Corr (the correlation between the AE and load) is first proposed to describe the

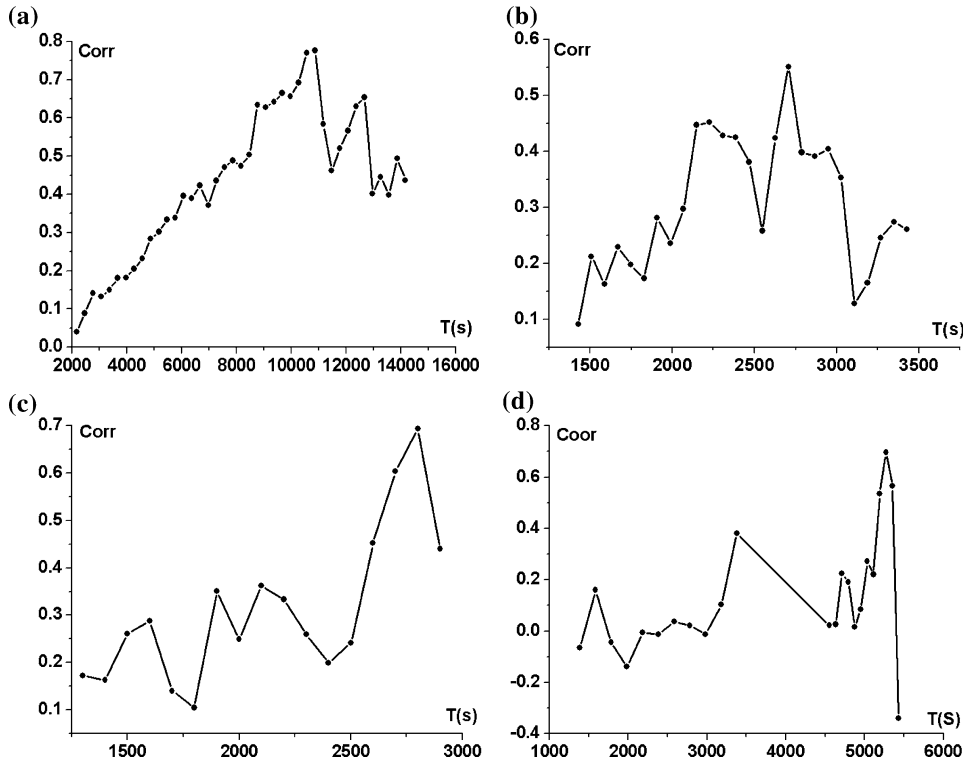

Figure 8
The correlation between the AE and load in rock fracture experiment: (a) gneiss G2, (b) gneiss G3, (c) sandstone S1, (d) sandstone S5.

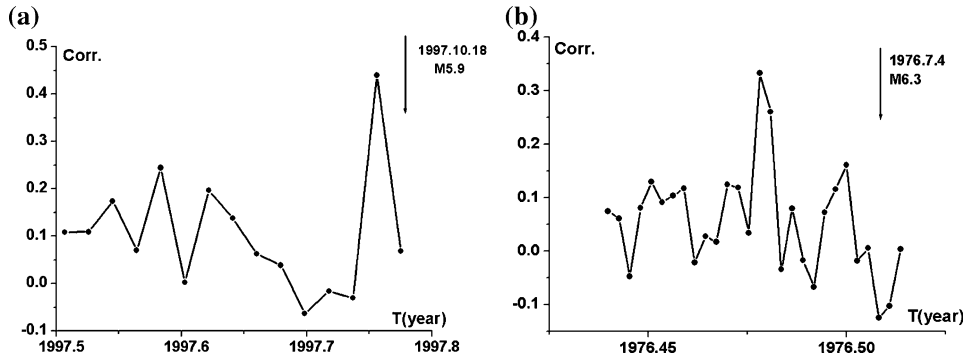

Figure 9
The correlation between the CFS and Benioff strain versus time before two strong earthquakes. (a) 1997.10.18, M 5.9, (39.60 N, 76.90 E), Jiashi Earthquake, Xinjiang Province. (b) 1976.7.4, M 6.3, (24.37 N, 98.50 E), Longling Earthquake, Yunan Province.

evolution of damage for the rock samples loading stage. The correlation between the CFS (Coulomb failure stress) and the Benioff strain before two strong earthquakes investigated reaches its peak point significantly is similar with LURR. This study brings new hopes to rock fracture and earthquake prediction.

Acknowledgments

The authors benefited greatly from anonymous reviewers in revising the manuscript. This research is supported by Natural Sciences Foundation of China (Grant No. 10232050, 10572140), MOST (Ministry of Science and Technology, China, Grant No.2004CB418406 and NO.2002CB412706), the Informatization Construction of Knowledge Innovation Projects of the Chinese Academy of Sciences "Supercomputing Environment Construction and Application" (INF105-SCE-2-02).

References

Beeler, N.M. and Lockner, D.A. (2003), *Why earthquakes correlate weakly with the solid Earth tides: Effects of periodic stress on the rate and probability of earthquake occurrence*, J. Geophys. Res. (in press).

Ben-Zion, Y. and Lyakhovsky, V. (2002), *Accelerated seismic release and related aspects of seismicity patterns on earthquake faults*, Pure Appl. Geophys. *159*, 2385–2412.

Bowman, D.D., Ouillon, G., Sammis, C.G., Sornette, A., and Sornette, D. (1998), *An observational test of the critical earthquake concept*, J. Geophys. Res. *103*, 24359–24372.

Bufe, C.G. and Varnes, D.J. (1993), *Predictive modeling of the seismic cycle of the greater San Francisco Bay region*, J. Geophys. Res. *98, B6*, 9871–9883.

Bufe, C.G., Nishenko, S.P., and Varnes, D.J. (1994), *Seismicity trends and potential for large earthquakes in the Alaska-Aleutian region*, Pure Appl. Geophys. *142*, 83–99.

Ellsworth, W.L., Lindh, A.G., Prescott, W.H., and Head, D.G. (1981), *The 1906 San Francisco earthquake and the seismic cycle*. In *Earthquake Prediction: An International Review (Maurice Ewing Series 4),* Washington, Amer. Geophys. Union, 126–140.

Grasso, J. and Sornette, D. (1998), *Testing self-organized criticality by induced seismicity,* J. Geophys. Res. *103, B12*, 29965–29987.

Harris, R.A. (1998), *Introduction to Special Section: Stress triggering, stress shadows, and implication for seismic hazard,* J. Geophys. Res. *103*, 24347–24358.

Huang, Y., Saleur, H., Sammis, C.G., and Sornette, D. (1998), *Precursors, aftershocks, criticality and self-organized criticality*, Europhys. Lett. *41,* 43–48.

Jaeger, J.C. and Cook, N.G.W. *Fundamentals of Rock Mechanics, 3rd Edition* (Chapman and Hall, 1979).

Keilis-Borok, V. *The lithosphere of the earth as a large nonlinear system*. In *Quo Vadimus: Geophysics for the Next Generation*, Geophys. Monogr. Ser. (eds. G. D. Garland and J. R. Apel) (AGU, Washington, D. C. (1990)) *60*, 81–84.

Knopoff, L., Levshina, T., Keilis-Borok, V.I., and Mattoni, C. (1996), *Increased long-range intermediate-magnitude earthquake activity prior to strong earthquakes in California,* J. Geophys. Res. *101*, 5779–5796.

Lockner, D.A., Byerlee, J.D., Kuksenko, V. *et al.* (1991), *Quasi-static fault growth and shear fracture energy in granite,* Nature *350* (7 MARCH) 39–42.

Lockner, D.A. (1993), *The role of emission in the study of rock failure,* Int. J. Rock Mech. Min. Sci. and Geomech. Asstr. *30* (7), 883–899.

LYAKHOVSKY, V., BEN-ZION, Y., and AGNON, A. (1997), *Distributed damage. faulting and friction*, J. Geophys. Res. *102*, 27,635–27,649.

MORA, P., PLACE, D., ABE, S., and JAUME, S., *Lattice solid simulation of the physics of fault zones and earthquakes: The model, results and directions*. In *Geocomplexity and the Physics of Earthquakes* (eds. Rundle, J.B., Turcotte, D.L. and Klein, W.) (AGU, Washington, DC, 2000), 105–125.

MORA, P. and PLACE, D. (2002), *Stress correlation function evolution in lattice solid elasto-dynamic models of shear and fracture zones and earthquake prediction,* Pure Appl. Geophys. *159*, 2413–2428.

RESERNBERG, P.A. and SIMPSON, R.W. (1992), *Response of regional seismicity to the static stress change produced by the Loma Prieta Earthquake,* Science *255*, 1687–1690.

RUNDLE, J.B. (1988a), *A physical model for earthquakes, 1. Fluctuations and interactions*, J. Geophys. Res. *93*, 6237–6254.

RUNDLE, J.B. (1988b), *A physical model for earthquakes, 2. Application to Southern California,* J. Geophys. Res. *93*, 6255–6274.

RUNDLE, J.B. (1989a), *Derivation of the complete Gutenberg-Richter magnitude frequency relation using the principle of scale invariance*, J. Geophys. Res. *94*, 12,337–12,342.

RUNDLE, J.B. (1989b), *A physical model for earthquakes: 3. Thermodynamical approach and its relation to nonclassical theories of nucleation*, J. Geophys. Res. *94*, 2839–2855.

RUNDLE, J.B., KLEIN, W., and GROSS, S. (1999), *A physical basis for statistical patterns in complex earthquake populations: models, predictions and tests,* Pure Appl. Geophys. *155*, 575–607.

RUNDLE, J.B., KLEIN, W., TIAMPO, K., and GROSS, S. (2000), *Precursory seismic activation and critical-point phenomena,* Pure Appl. Geophys. *157*, 2165–2182.

SAMMIS, C.G. and SMITH, S.W. (1999), *Seismic cycles and the evolution of stress correlation in cellular automation models of finite fault networks*, Pure Appl. Geophys. *155*, 307–334.

SORNETTE, A. and SORNETTE, D. (1990), *Earthquake rupture as a critical point: Consequences for telluric precursors*, Tectonophysics *179*, 327–334.

SORNETTE, D. (1992), *Mean-field solution of a Block-spring Model of Earthquake*, J. Phys. I, France *2*, 2089–2096.

SORNETTE, D. and SAMMIS, C.G. (1995), *Complex critical exponents from renormalization group theory of earthquake prediction*, J. Phys. I, France *5*, 607–619.

TOMILIN, N.G., DAMASKINSKAYA, E.E., and KUKSENKO, V.S. (1994), *Formation of a fracture focus during the deformation of heterogeneous materials (Granite),* Phys. Solid State *36* (10), 1649–1653.

TURCOTTE, D.L., NEWMAN, W.I., and SHCHERBAKOV, R. (2002), *Micro- and macroscopic models of rock fracture*, Geophys. J. Int. *152*, 718–728.

VIDALI, J.E., AGNEW, D.C., JOHNSTON, M.J.S., and OPPENHEIMER, D.H. (1998), *Absence of earthquake correlation with earth tides: An indication of high preseismic fault stress rate*, J. Geophys. Res. *103*, 24567–24572.

WANG, Y.C., YIN, C., MORA, P. YIN, X.C. and PENG, K.Y., *Spatiotemporal scanning and statistical test of the accelerating moment release (AMR) model using Australian earthquake data,* 3rd APEC Cooperation for Earthquake Simulation Workshop Proceedings (eds. A. Donnellan and Peter Mora Goprint, Brisbane, 2003), 265–270.

WEATHERLEY, D., MORA, P., and XIA, M. (2002), *Long-range automaton models of earthquakes: Power-law accelerations, correlation evolution, and mode switching*, Pure Appl. Geophys. *159,* 2469–2490.

XIA, M.F., WEI, Y.J., KE, F.J., and BAI, Y.L. (2002), *Critical sensitivity and transscale fluctuations in catastrophic rupture*, Pure Appl. Geophys. *159*, 2491–2510.

YIN, X.C. and YIN, C. (1991), *The precursor of instability for nonlinear systems and its application to earthquake prediction*, Science in China *34*, 977–986.

YIN, X.C. (1993), *New approach to earthquake prediction*, Preroda (Russia's "Nature"). *1*, 21–27 (in Russian).

YIN, X.C., YIN, C., and CHEN, X.Z. (1994), *The Precursor of instability for nonlinear system and its application to earthquake prediction-the Load-Unload Response Ratio theory*. In *Non-linear Dynamics and Predictability of Geophysical Phenomena* (eds. Neuman, W.I., Gabrelov, A. M., and Turcotte, D.L.) (AGU Geophysical Monograph *83*, 1994), 55–60.

YIN, X.C., CHEN, X.Z., SONG, Z.P., and YIN, C. (1995), *A new approach to earthquake prediction – The Load-Unload Response Ratio (LURR) theory*, Pure Appl. Geophys. *145*, 3/4, 701–715.

YIN, X.C., CHEN, X.Z., SONG, Z.P., and WANG, Y.C. (1996), *The temporal variation of LURR in Kanto and other regions in Japan and its application to earthquake prediction*, Earthq. Res. in China *10*, 381–385.

YIN, X.C., WANG, Y.C., PENG, K.Y., BAI, Y.L., WANG, H., and YIN, X.F. (2000), *Development of a new approach to earthquake prediction: Load/Unload Response Ratio (LURR) theory*, Pure Appl. Geophys. *157*, 1923–1941.

YIN, X.C., MORA, P., PENG, K.Y., WANG, Y.C., and WEATHERLY, D. (2002), *Load-Unload Response Ratio and Accelerating Moment/Energy Release, critical region scaling and earthquake prediction,* Pure Appl. Geophys. *159*, 2511–2524.

ZHONG, HUAI, XU, SU, YUN, WANG, YANXIANG, YU, and AJIA, GAO (1995), *The basic features of the tectonic stress filed in China mainland, The developments of scientific and observational technology in earth and space* (eds. Yuntai Chen) (Earthquake Press), 312–318 (in Chinese).

ZHANG, X.H., XU, X.H., XIA, M.F. and BAI, Y.L. (2004), *Critical sensitivity in driven nonlinear threshold systems*, Pure Appl. Geophys. *161*, 1931–1944.

(Received December 13, 2004, revised August 10, 2005, accepted August 12, 2005)
Published Online First: December 20, 2006